Central Lancashire Online Knowledge (CLoK)

Title	Spectroscopic and quartz crystal microbalance (QCM) characterisation of protein-based MIPs
Type	Article
URL	https://clok.uclan.ac.uk/14368/
DOI	https://doi.org/10.1016/j.snb.2014.09.053
Date	2015
Citation	El-Sharif, H.F., Aizawa, H. and Reddy, Subrayal M orcid iconORCID: 0000-0002-7362-184X (2015) Spectroscopic and quartz crystal microbalance (QCM) characterisation of protein-based MIPs. Sensors and Actuators, B: Chemical, 206. pp. 239-245. ISSN 0925-4005
Creators	El-Sharif, H.F., Aizawa, H. and Reddy, Subrayal M

It is advisable to refer to the publisher's version if you intend to cite from the work. https://doi.org/10.1016/j.snb.2014.09.053

For information about Research at UCLan please go to http://www.uclan.ac.uk/research/

1 **Spectroscopic and Quartz Crystal Microbalance (QCM) Characterization of Protein-**

2 **based MIPs**

3

4 Hazim F. EL-Sharif[1],Hidenbou Aizawa[2], Subrayal M. Reddy[1*]

5

6 [1]Department of Chemistry, Faculty of Engineering and Physical Sciences, University of

7 Surrey, Guildford, Surrey, GU2 7XH, UK

8 [2]Institute for Environmental Management Technology, National Institute of Advanced
9 Industrial Science and Technology (AIST), 1-1 Higashi, Tsukuba 305-8565, Japan

10

11 ***Corresponding Author**

12 Tel : +44 (0) 1483686396, **s.reddy@surrey.ac.uk**

13

14 **Abstract**

15 We have studied acrylamide-based polymers of varying hydrophobicity (acrylamide, AA; N-

16 hydroxymethylacrylamide, NHMA; N-isopropylacrylamide, NiPAm) for their capability of

17 imprinting protein. Rebinding capacities (Q) from spectroscopic studies were highest for

18 bovine haemoglobin (BHb) MIPs based on AA, $Q = 4.8 \pm 0.21 <$ NHMA, $Q = 4.3 \pm 0.32 <$

19 NiPAm, $Q = 3.6 \pm 0.45$, while also demonstrating low selectivities for non-template proteins

20 ($<30 \pm 5\%$), with the exception of bovine serum albumin (BSA, $>76 \pm 0.5\%$). When applied

21 to the QCM sensor as thin-film MIPs, NHMA MIPs were found to exhibit best discrimination

22 between MIP and non-imprinted control polymer (NIP) in the order of NiPAm < AA <

23   NHMA. The extent of template removal and rebinding, using both crystal impedance and

24   frequency measurements, demonstrated that 10% (w/v):10% (v/v) sodium dodecyl

25   sulphate:acetic acid (pH 2.8) was efficient at eluting template BHb (with $80 \pm 10\%$ removal).

26   Selectivity studies of NHMA BHb-MIPs revealed higher adsorption and selective recognition

27   properties to BHb (64.5 kDa) when compared to non-cognate BSA (66 kDa), myoglobin

28   (Mb, 17.5 kDa), lysozyme (Lyz, 14.7 kDa) thaumatin (Thau, 22 kDa) and trypsin (Tryp, 22.3

29   kDa). The QCM gave frequency shifts of $\sim 1500 \pm 50$ Hz for template BHb rebinding in both

30   AA and NHMA MIPs, whereas AA-based MIPs exhibited an interference signal of $\sim 2200 \pm$

31   50 Hz for non-cognate BSA in comparison to a $\sim 500 \pm 50$ Hz shift with NHMA MIPs. Our

32   results show that NHMA-based hydrogel MIP are superior to AA and NIPAM..

33

1. Introduction

1. Introduction

In recent years, molecularly imprinted polymers (MIPs) have allowed selective extractions that rival immunoaffinity-based separations, and have shown clear advantages over real antibodies for sensor applications: they are easy to fabricate, intrinsically stable, robust, and are able to operate in extreme environments [1], [2] and [3]. MIPs could provide an alternative, inexpensive, fast, and efficient diagnostic method for highly sensitive analytical procedures within the pharmaceutical area [3].

When imprinting complex bio-macromolecules some of the most significant drawbacks in MIP technology are the unprecedented degree of influence that the variation in pH [4], ionic strength and local matrix effects all have on the gel properties [5], [6], [7] and [8]. This can affect the three dimensional shape and chemical characteristics of the template molecule during polymerisation. This is particularly true when imprinting large bio-macromolecules such as proteins. Proteins are relatively labile, and have variable conformations which are sensitive to solvent environments, pH and temperature, all of which present a variety of challenges [5]. It has been thought that low imprinting capacities associated with bio-macromolecules could be caused by the use of charged functional monomers causing non-specific electrostatic interactions [5]. Moreover, as with antibodies, MIPs have also shown a degree of cross-selectivity, in that they can bind molecules similar to the native template and cause non-specific binding. It is thought that this is due in part to an excess of functional monomer molecules being randomly distributed and frozen within the imprinted cavity during polymerisation that have an affinity for non-template molecules [3] and [9]. Thus, more sophisticated monomers capable of forming better, stronger and more stable

59 interactions that offer better positioning and complementary functionality are widely being

60 sought. Once these parameters are optimised, application to biosensors and analysis of actual

61 biological samples would be more realistic [6], [10], [11] and [12].

62

63 Biosensors for proteins are currently expensive to develop because they require the use of

64 expensive antibodies [3] and [13]. However, as MIPs are becoming more and more promising

65 as viable alternatives to natural receptors new MIP-based sensor strategies are being

66 developed [3]. The main advantage of biosensors is the ability to sample outside the

67 laboratory environment with minimal user input. One important part of bio-sensing is

68 transducers, which monitor the reaction between bio-selector and analyte. Among various

69 physical transducers (electrochemical, peizoelectric, etc.), mass sensitive devices such as

70 surface acoustic wave (SAW), surface plasmon resonance (SPR) and quartz crystal

71 microbalance (QCM) have become popular for sensing applications [14], [15], [16] and [17].

72

73 Following the thorough analysis of QCM systems for use in fluids over the past 2 decades,

74 this has allowed for more esoteric applications including bio-sensing [16]. In most cases

75 quartz resonators are integrated to oscillator circuits to form a QCM for micro weighing

76 applications. Normally, an equivalent circuit model is fitted to the impedance curve, and the

77 obtained parameters can be used for calculating the resonant frequency and dissipation (D) of

78 the quartz crystal i.e. mass and viscoelastic properties of the deposited layers [15] and [16].

79 Determining the impedance curve has many advantages; first and foremost it has expanded

80 the range of measurable parameters from rigid thin films, to biologically relevant films of

81 "soft" viscoelastic material. These QCM couplings have been widely used for biomaterials

82 and biosensor studies [10], [12], [16], [18] and [19], where surface confined bio-molecular

interactions have provided an insight into dissolution of polymer coatings, DNA

hybridisation, cell response to pharmacological substances, molecular interactions of drugs

and their delivery. The QCM has also been utilised as an immunosensor, where analytes are

recognised by antibodies, which are immobilised on a thin layer deposed on a crystal surface.

Resulting mass changes are transformed into an electronically measurable quantity. The

objective behind the majority of QCM research is to use sensor technology to develop a rapid

method for the measurement of bio-molecular affinity reactions, and an in-depth analysis of

electrochemical deposition, adsorption and reaction mechanisms of polymers coated on

electrodes as 'thin films' [10], [12], [18], [19] and [20].

The focus of this paper is the tailoring of QCM electrode surface chemistry (i.e. specialised

polymer coatings), with a view that these devices can discriminate proteins for bio-sensing

and basic surface-molecular interaction studies. In this work, we demonstrate the application

of the QCM technique to distinguish between the behaviour of MIPs and NIPs in the

presence of cognate and non-cognate proteins. Bovine haemoglobin (BHb, 64.5 kDa) was

chosen as a model protein for its well-known function in the vascular system as a carrier of

oxygen, also in aiding the transport of carbon dioxide and regulating blood pH [3] and [13].

Bovine serum albumin (BSA, 66 kDa), a non metalloprotein of similar molecular weight to

BHb, served to test the selectivity of the BHb-MIP to BSA compared to template BHb, and

was compared across a family of acrylamide-based polymer hydrogels.

2. Experimental

2.1. Materials

5

106

107   Acrylamide (AA), N-hydroxymethylacrylamide (NHMA), N-iso-propylacrylamide (NiPAm),

108   N,N′-methylenebisacrylamide (bis-AA), ammonium persulphate (APS), N,N,N′,N′-

109   tetramethylethylenediamine (TEMED), sodium dodecyl-sulphate (SDS), glacial acetic acid

110   (AcOH), bovine haemoglobin (BHb), bovine serum albumin (BSA), hen egg-white lysozyme

111   (Lyz), thaumatin from Thaumatococcus danielii (Thau), bovine pancreatic trypsin (Tryp) and

112   equine heart myoglobin (Mb) were all purchased from Sigma–Aldrich, Poole, Dorset, UK.

113   Sieves (75 μm) were purchased from Endecotts Ltd. and Inoxia Ltd., UK. AT-cut quartz

114   crystal pieces (9 MHz fundamental resonance) with gold-on-chrome electrodes were supplied

115   by Nihon Dempa Kogyo Company Ltd. (Tokyo, Japan).

116

117   2.2. HydroMIP preparations

118

119   Hydrogel MIPs were synthesised by separately dissolving AA (54 mg), NHMA (77 mg),

120   NiPAm (85.6 mg) and bis-AA as cross-linker (6 mg), (8.5 mg) and (9.5 mg), respectively

121   along with template protein (12 mg) in 960 μL of MilliQ water. The solutions were purged

122   with nitrogen for 5 min, followed by an addition of 20 μL of a 10% (w/v) APS solution and

123   20 μL of a 5% (v/v) TEMED solution. Polymerisation occurred at room temperature (RT, 22

124   ± 2 °C) giving total gel densities (%T) of 6%T, AA/bis-AA (w/v); 8.5%T, NHMA/bis-AA

125   (w/v); 9.5%T, NiPAm/bis-AA (w/v), and final crosslinking densities (%C) of 10%C (9:1,

126   w/w) for all hydrogels.

127

128 For every MIP created a non-imprinted control polymer (NIP) was prepared in an identical

129 manner but in the absence of protein. After polymerisation, the gels were granulated

130 separately using a 75 μm sieve. Of the resulting gels, 500 mg were transferred into 1.5 mL

131 centrifuge Eppendorf tubes and conditioned by washing with five 1 mL volumes of MilliQ

132 water followed by five 1 mL volumes of 10% (w/v):10% (v/v) SDS:AcOH (pH 2.8) and

133 another five 1 mL volume washes of MilliQ water to remove any residual 10% (w/v):10%

134 (v/v) SDS:AcOH eluent and equilibrated the gels. Each wash step was followed by a

135 centrifugation, whereby the gels were centrifuged using an Eppendorf mini-spin plus

136 centrifuge for 3 min at 6000 rpm (RCF: $2419 \times g$). All supernatants were collected for

137 analysis by spectrophotometry to verify the extent of template removal. It should be noted

138 that the last water wash and eluent fractions were not observed to contain any protein.

139 Therefore we are confident that any remaining template protein within the MIPs did not

140 continue to leach out during the rebinding studies.

141

142 2.3. Rebinding studies

143

144 Once the gels (500 mg) were equilibrated, a 1 mL template protein solution prepared in

145 MilliQ water containing 3 mg of protein was added to the target MIPs and NIP controls and

146 was allowed to associate at RT (22 ± 2 °C) for 20 min. Selectivity studies were also

147 conducted to assess the relative imprinting factor of the original protein template. This was

148 achieved by loading non-cognate proteins on a BHb imprinted gel. Gels were then washed

149 with four 1 mL volumes of MilliQ water. Each reload and wash step for all MIPs and NIP

150 controls was followed by centrifugation at 6000 rpm (RCF: $2419 \times g$) for 3 min. All

151 supernatants were collected for analysis by spectrophotometry.

7

152

153 2.4. Spectrophotometric analysis

154

155 Calibration curves in MilliQ water and 10% (w/v):10% (v/v) SDS:AcOH were prepared for

156 BHb, BSA, Lyz, Tryp and Mb. Spectral scans revealed peak wavelengths for BHb in MilliQ

157 water and 10% (w/v):10% (v/v) SDS:AcOH to be 405 nm and 395 nm, respectively. Peak

158 wavelengths for BSA in MilliQ water and 10% (w/v):10% (v/v) SDS:AcOH were found to be

159 288 nm and 290 nm respectively. Peak wavelengths for Lyz in MilliQ water and 10%

160 AcOH:SDS were found to be 291 nm and 296 nm respectively. Peak wavelengths for Tryp in

161 MilliQ water and 10% (w/v):10% (v/v) SDS:AcOH were found to be 293 nm. Peak

162 wavelengths for Mb in MilliQ water, 10% (w/v):10% (v/v) SDS:AcOH were found to be 410

163 nm, and 396 nm respectively. Analysis and subsequent determination of protein

164 concentration in appropriate media was performed at specific peak wavelengths using a UV

165 mini-1240 CE spectrophotometer (Shimadzu Europa, Milton Keynes, UK).

166

167 2.5. Quartz crystal microbalance (QCM) analysis of thin film MIPs

168

169 QCM crystals were sealed and air capped (single-sided) with PVC glue in-order to prevent

170 short circuiting when the QCM was submerged in solution [10]. Poly AA, NHMA and

171 NiPAm gels for BHb were synthesised using the hydrogel production procedures outlined in

172 Section 2.2. Before polymerisation, MIPs and NIPs were deposited as thin films onto the

173 capped QCM crystals. Thin-films were achieved by beading and compressing 10 μL of the

174 polymerising solutions directly onto the crystals. QCM frequency and impedance

175 measurements were taken using an Agilent 4194A Impedance Analyser. An in-house written

176 QBasic programme was used to drive the analyser and collect series resonance frequency and

177 impedance data in real time.

178

179 2.5.1. Elution and rebinding studies

180

181 MIP and NIP polyAA thin-film capped crystals were firstly immersed in MilliQ water,

182 followed by 10% (w/v):10% (v/v) SDS:AcOH in order to remove imprinted protein primarily

183 from the surface of the polymer. This was followed by another submersion in MilliQ water to

184 remove any residual surfactant and to re-condition the hydrogel. After subsequent

185 stabilisation of the QCM response, template protein was reloaded by immersing the QCM in

186 a 3 mg/mL BHb solution and the response trace was recorded at RT (22 ± 2 °C).

187

188 2.5.2. Selectivity studies

189

190 Continuous real-time scans were conducted in-order to assess characteristic impedance

191 changes of the gels during surface exposure to wash, elute and protein rebinding conditions.

192 During a typical run, the MIP thin-film capped crystals were submerged sequentially in

193 various solutions such as 10% (w/v):10% (v/v) SDS:AcOH, MilliQ water or 3 mg/mL protein

194 solutions (cognate BHb and non-cognate BSA, Thau, Lyz and Tryp) for a set time of 5 min

195 each, and crystal impedance and frequency responses were recorded at RT (22 ± 2 °C). The

196 latter procedure was followed for AA, NiPAm and NHMA based MIP hydrogels for BHb.

197

198   3. Results and discussion

199   3.1. MIP selectivity

200   The molecular imprinting effect is characterised by the rebinding capacity (Q) of protein to

201   the gel polymer (mg/g) exhibited by the protein-specific MIP and the control NIP, and is

202   calculated using Eq. (1), where Ci and Cr are the initial protein and the recovered protein

203   concentrations (mg/mL) respectively (which specifies the specific protein bound within the

204   gel), V is the volume of the initial solution (mL), and g is the mass of the gel polymers (g).

205

206    $$Q = \frac{[C_i - C_r]V}{g}$$ (1)

207

208   Fig. 1A shows the rebinding capacities and imprinting factors of polyacrylamide (polyAA)

209   MIP and NIPs for several different proteins. The internal measure of the imprinting factor

210   between MIP and NIP serves to demonstrate that the MIP possesses selective cavities for the

211   rebinding of template molecule compared to NIP controls. It can clearly be seen that there is

212   a distinctive rebinding capacity variation for each imprinted protein template within a

213   polyAA MIP. This has previously been attributed to protein size, cross-linking density, and

214   the initial degree of association within the polymer matrix [4].

215   Gels based on N-hydroxymethylacrylamide (NHMA) exhibited similar rebinding trends,

216   whereas poly-N-isopropylacrylamide gels (polyNiPAm) demonstrated lower rebinding

217   capacities. Thus, bulk gel characterisation revealed the highest rebinding capacities for BHb

218   MIPs based on polyAA (Q = 4.8 ± 0.21), followed by polyNHMA (Q = 4.3 ± 0.32),

10

219   polyNiPAm (Q = 3.6 ± 0.45). These gel imprinting trends are in agreement with those

220   previously published [4], [9] and [10].

221

222   Selectivity studies were also conducted to confirm a BHb specific imprinting effect and to

223   assess the relative imprinting factor of cross-selective binding profiles. The cross-reactivity of

224   the BHb-imprinted MIPs for non-cognate proteins was quantified using relative imprinting

225   factors (k), Eq. (2), where IFBHb is the imprinting factor for BHb, and is calculated by IF =

226   [Ci − Cr]MIP/[Ci − Cr]NIP, and IFx is the imprinting factor of the cross-reacting non-

227   cognate proteins on a BHb MIP. For the template BHb k = 1, and for non-cognate proteins

228   that are less-specific for the BHb MIP, k < 1.

229

230   $$k = \frac{\text{IF}_{BHb}}{\text{IF}_x} \qquad\qquad (2)$$

231   The data (Fig. 1B) suggests that both non-cognate trypsin (Tryp) and lysozyme (Lyz) proteins

232   have relatively low affinities for the BHb-specific MIP, k ≈0.2 ± 0.05. However, bovine

233   serum albumin (BSA), which is a similar size to BHb, exhibited a high degree of interference

234   binding (cross selectivity) resulting in high k values of 0.65 ± 0.05. Myoglobin (Mb) also

235   exhibited some degree of cross-selectivity; this can be attributed to the size of Mb, which is a

236   quarter that of BHb (17.5 kDa), and its similarity to a single BHb sub-unit [4]. Interestingly

237   though, when reversed, a polyAA BSA-MIP exposed to non-target BHb protein had

238   relatively low affinity. It would appear that BSA has a high ability to bind non-specifically to

239   a BHb MIP, whereas BHb does not exhibit the same ability within a BSA MIP.

240

11

241   Competitive binding studies using a 50:50 mixture of BHb:BSA (3 mg/mL total) on a MIP-

242   BHb were also conducted (Fig. 1B). The addition of BSA caused an obvious capacity

243   decrease of BHb binding on the BHb-MIP, suggesting that the rebinding of BHb was

244   displaced by the competing BSA or by protein-protein interactions [21]. As the size,

245   structure, and specificity of the imprinted cavities should be in favour of the BHb template, it

246   is rational that the addition of BSA as a competing protein would not bind to the BHb-

247   specific imprinted cavities. Gai et al. previously demonstrated that BSA does not bind

248   specifically to a BHb MIP, but rather displaces the non-specific recognition sites of cavities

249   and the nonspecific binding of BHb to BHb-MIP [21]. Moreover, although BSA and BHb

250   share similar sizes (66 kDa and 64.5 kDa, respectively), it should be noted that BSA has a pI

251   of 4.6 and BHb a pI of (6.8–7.0). Since competitive binding was performed under MilliQ

252   water (pH 5.4), conditions are in favour of BSA [21] and [22]. Above its pI, BSA becomes

253   negatively charged and the groups exist as single bondNH2 and single bondCOO−, this

254   overall negative net charge induces more favourable and complementary hydrogen bonding

255   interactions, resulting in increased specific as well as non-specific binding [4].

256

257   3.2. QCM sensor application of MIPs

258   Thin film BHb MIPs were prepared on the surface of a QCM chip and the sensor was

259   exposed sequentially to MilliQ water, 10% (w/v):10% (v/v) SDS:AcOH and 3 mg/mL protein

260   solutions at RT (22 ± 2 °C). We have previously published on the thickness of the thin films

261   on sensor chips with an average thickness of 138 ± 9 nm [6]. Given that for a 9 MHz crystal

262   the shear wave decay length is 250 nm at RT [23], we are within the sensing region of the

263   QCM to measure both bulk and surface effects within the MIP film.

264

265   Fig. 2A and B shows the QCM impedance and frequency responses following immersion in a

266   solution of 10% (w/v):10% (v/v) SDS:AcOH in order to remove imprinted protein from the

267   surface of the polymer. Previous investigations have shown that optimum conditions for

268   protein removal of up to 80% have been achieved using 10% (w/v):10% (v/v) SDS:AcOH

269   [9]. Using this acid/surfactant combination the positively charged protein attaches to the

270   negatively charged surface of SDS micelles and disrupts the hydrophobic bonds. Since there

271   is a significant shift in both resonance frequency and impedance it can be assumed that some

272   of the BHb imprinted template has been successfully removed from the MIP.

273   It is worth noting the two distinct differences in the impedance response when compared with

274   the frequency response. Firstly, the impedance response has much reduced noise in the signal

275   in contrast to the frequency response. Secondly, there are significant additional transitions

276   (e.g. at 350 and 650 s) in the signal which are being observed in the Z response, but not in the

277   frequency response. It has been suggested that whereas the frequency response predominately

278   demonstrates the QCM mass response only within an adlayer, the electrical impedance gives

279   a combination response of the mass effect as well as subsequent changes in the viscoelasticity

280   of the adlayer possibly due to molecular relaxations within the adsorbed layer over a longer

281   timescale following initial immersion [23], [24] and [25].

282

283   After subsequent stabilisation of the QCM response, the template BHb was then reloaded by

284   immersing the QCM in a 3 mg/mL BHb solution and the response trace recorded. Fig. 2C and

285   D compares the final QCM impedance and frequency responses to template BHb exposure of

286   each MIP and its corresponding NIP. It can be seen that upon addition of a 3 mg/mL BHb

287   solution to the BHb MIP caused significant QCM responses compared with NIP thin-film

288   hydrogels. This suggests that MIP thin-film gels are affected by specific binding of target

13

289   BHb. This distinct difference between responses exhibited by MIP and the NIP control

290   strongly supports that binding and elution of target protein gave rise to distinct impedance

291   transitions. The 200 ± 50 Hz frequency shift observable by both MIP and NIP during the

292   initial loading step (Fig. 2D) is suggestive of a solution viscosity effect.

293

294   Real time impedance response following sequential immersion in solutions of BHb, 10%

295   (w/v):10% (v/v) SDS:AcOH and BSA were also measured. Three distinct types of responses

296   were observed depending on the acrylamide-based monomer used. The key difference

297   between the polymers is their hydrophilicity dictated by the hydrophilic hydroxyl group in

298   NHMA and the hydrophobic isopropyl group in NiPAm. AA sits between the two in degree

299   of hydrophilicity (polyNHMA > polyAA > polyNiPAm), which agrees with the order of best

300   performance of the polymers as BHb MIPs in previous QCM studies [10]. Fig. 3 compares

301   the final QCM response to cognate and non-cognate protein exposure of each MIP with its

302   corresponding NIP. Interestingly, the NiPAm MIP and NIP both show a near zero frequency

303   response to template BHb and non-cognate BSA, indicating that NiPAm is equally

304   unselective for both proteins as is the control non-imprinted polymer. The non-response of

305   NiPAm to either BHb or BSA suggests that there is a resistance to either protein to bind to

306   the polymer. The striking difference in selectivities between cognate and non-cognate

307   proteins for NHMA and AA suggests that the hydroxyl group in NHMA plays a significant

308   role in the selective binding of BHb and the lack of binding of BSA.

309   Moreover, variations of the series resonance frequency demonstrated to be highly dependent

310   on the test solution used (Fig. 4A). The impedance data is presented here because in

311   comparison to the frequency response, there is much reduced noise in the signal following

312   each solution phase immersion. It can be seen that MIP thin-films exposed to a 10%:10%

14

313 (v/v) SDS:AcOH solution exhibited an immediate significant decrease in impedance (500 ±

314 100 Ω); this is possibly due to the increase in the viscosity of the solution caused by the

315 presence of SDS micelles in the solution. Moreover, it can clearly be seen that the

316 introduction of non-template BSA also exhibits an impedance response within the poly AA

317 MIP, suggesting some non-specific binding within the BHb-HydroMIP. Thus, there is a high

318 degree of cross-selectivity present for our AA-based MIPs (>70%), and this interference is

319 absent when NHMA-based MIPs are used (<20%) as seen in Fig. 3.

320 To further test the BHb-MIP selectivity, we investigated the rebinding of template BHb after

321 exposing the MIP with non-target BSA. The resulting quantified imprinting effect of BHb for

322 polyAA MIP thin-film gels can be seen in the impedance responses (Fig. 4B). The

323 comparison demonstrates that both HydroMIP and HydroNIP films act differently under

324 water wash, elution and load (solution immersion) treatments following BSA loading. It can

325 be seen that when non-target BSA is loaded first, the QCM impedance response is now

326 negligible. Interestingly, impedance responses are also almost negligible when BHb is

327 introduced after prior exposure to BSA. Although the loaded BSA did not associate

328 specifically with the BHb-MIP thin-film surface, an interesting and lasting effect inhibits

329 BHb from easily binding to recognition sites. Indeed, BSA is similar to the template BHb in

330 size, but the spatial arrangement of the effective groups on its exterior are different from

331 BHb, and the recognition sites in the BHb-MIP cavities are not complementary in shape to

332 BSA [22]. Therefore, little to no selectivity of BSA on BHb-MIPs should be expected.

333 Therefore, in the case of AA-based MIPs, the inhibition effect is most likely due to the ability

334 of BSA to exhibit protein binding on the MIP surface but not within cavities. Formation of a

335 BSA biolayer above (but not within) the cavities would block subsequent cavity-selective

336 MIP binding for its cognate protein [22]. This is further indication that BHb-MIPs distinguish

337 proteins not only based on molecular size, but also on the synergistic effect of shape memory,

338   and multiple weak hydrogen bonding interactions specific to template protein in

339   macromolecular recognition [21], [22] and [26].

340

341   Moreover, further studies to interrogate the recognition capabilities of MIPs were carried out

342   using a range of non-metalloproteins chosen for their different sizes and functionalities

343   compared to BHb, BSA and Mb. Of these proteins: lysozyme (Lyz), a glycoside hydrolase

344   enzyme (14.7 kDa) that is part of the innate immune system, and exists as a natural form of

345   protection from pathogens like Salmonella, E. coli, and Pseudomonas [9], [10] and [27].

346   Thaumatin (Thau), a sweetener or flavour modifier (22 kDa) often used in crystallisation

347   studies due to its ease of use and crystal formation [27]. Trypsin (Tryp), a serine protease

348   enzyme or proteinase 'digestive enzyme' (23.8 kDa) commonly imprinted within MIPs [9],

349   [10] and [27]. Fig. 5 shows that the BHb-MIPs based on all three polymers (AA, NHMA, and

350   NiPAm) are essentially non-responsive to the addition of the three smaller proteins Thau, Lyz

351   and Tryp respectively. An average NIP response was calculated based on all three polymers

352   and used as an illustration to demonstrate the negligible responses exhibited by the MIP

353   properties. The negligible responses exhibited by the QCM sensor concur with the qualitative

354   data and confirm that these small proteins exhibit no selective specific/non-specific binding

355   characteristics to a BHb-imprinted MIP.

356

357   4. Conclusions

358   A family of acrylamide-based MIPs have been characterised for their imprint efficiency using

359   spectrophotometric and QCM sensor techniques for biosensor development. Varied rebinding

360   capacities and relative imprinting factors have been achieved using bulk characterisation. We

361   have demonstrated that MIP selectivity is a function of the hydrophilicity of the acrylamide

362   monomer used to form the MIP. Three distinct types of QCM responses were observed

363   depending on the acrylamide used (polyNHMA > polyAA > polyNiPAm), which agrees with

364   the order of best performance of the polymers in previously published QCM studies. The

365   selectivity of BHb-MIP for BHb and BSA was also compared via QCM, along with several

366   other proteins. Results demonstrated BHb-MIP to have better selective adsorption and

367   recognition properties to BHb than BSA when using the hydrophilic NHMA as a MIP

368   polymer matrix. Therefore, the QCM sensor was able to indicate MIP surface activity and

369   provide physical interpretation in terms of hydrophilicity of the polymer matrix that forms the

370   MIP and protein selectivity. Our QCM sensor also has the ability to assess the extent of

371   specific protein binding by sensing surface-specific bound cognate protein to MIPs compared

372   to non-imprint NIP controls. We expect, once fully developed, that the benefits of sensitivity,

373   specificity and stability of MIPs coupled with discriminatory techniques, such as QCM, will

374   be crucial to the future impact of portable diagnostics for personal healthcare and use by

375   health professionals. The technology also presents major potential benefits to environmental

376   and food monitoring.

377

381

382   References

17

383 [1] S. Pradhan, M. Boopathi, O. Kumar, A. Baghel, P. Pandey, T.H. Mahato, B. Singh, R.

384 Vijayaraghavan, Molecularly imprinted nanopatterns for the recognition of biological warfare

385 agent ricin Biosens. Bioelectron., 25 (2009), pp. 592–598

386 [2] D.R. Kryscio, N.A. Peppas Critical review and perspective of macromolecularly

387 imprinted polymers Acta Biomater., 8 (2012), pp. 461–473

388 [3] M.J. Whitcombe, I. Chianella, L. Larcombe, S.A. Piletsky, J. Noble, R. Porter, A. Horgan

389 The rational development of molecularly imprinted polymer-based sensors for protein

390 detection Chem. Soc. Rev., 40 (2011), pp. 1547–1571

391 [4]H.F. El-Sharif, Q.T. Phan, S.M. Reddy Enhanced selectivity of hydrogel-based

392 molecularly imprinted polymers (HydroMIPs) following buffer conditioning Anal. Chim.

393 Acta, 809 (2014), pp. 155–161

394 [5] E. Verheyen, J.P. Schillemans, M. van Wijk, M. Demeniex, W.E. Hennink, C.F. van

395 Nostrum Challenges for the effective molecular imprinting of proteins Biomaterials, 32

396 (2011), pp. 3008–3020

397 [6] S.M. Reddy, D.M. Hawkins, Q.T. Phan, D. Stevenson, K. Warriner Protein detection

398 using hydrogel-based molecularly imprinted polymers integrated with dual polarisation

399 interferometry Sens. Actuators B: Chem., 176 (2013), pp. 190–197

400 [7] S.A. Piletsky, N.W. Turner, P. Laitenberger Molecularly imprinted polymers in clinical

401 diagnostics – future potential and existing problems Med. Eng. Phys., 28 (2006), pp. 971–977

402 [8] M.E. Byrne, V. Salian Molecular imprinting within hydrogels. II. Progress and analysis

403 of the field Int. J. Pharm., 364 (2008), pp. 188–212

404

405   [9] D.M. Hawkins, D. Stevenson, S.M. Reddy Investigation of protein imprinting in

406   hydrogel-based molecularly imprinted polymers (HydroMIPs) Anal. Chim. Acta, 542 (2005),

407   pp. 61–65

408

409   [10] S.M. Reddy, Q.T. Phan, H. El-Sharif, L. Govada, D. Stevenson, N.E. Chayen

410   Protein crystallization and biosensor applications of hydrogel-based molecularly imprinted

411   polymers Biomacromolecules, 13 (2012), pp. 3959–3965

412   [11] P.A. Lieberzeit, R. Samardzic, K. Kotova, M. Hussain MIP sensors on the way to

413   biotech application: selectivity and ruggedness Proc. Eng., 47 (2012), pp. 534–537

414   [12] B.B. Prasad, I. Pandey Molecularly imprinted polymer-based piezoelectric sensor for

415   enantio-selective analysis of malic acid isomers Sens. Actuators B: Chem., 181 (2013), pp.

416   596–604

417   [13]S.M. Reddy, G. Sette, Q. Phan Electrochemical probing of selective haemoglobin

418   binding in hydrogel-based molecularly imprinted polymersElectrochim. Acta, 56 (2011), pp.

419   9203–9208

420   [14]G.N.M. Ferreira, A. da-Silva, B. Tomé Acoustic wave biosensors: physical models and

421   biological applications of quartz crystal microbalance Trends Biotechnol., 27 (2009), pp.

422   689–697

423   [15] T.M.A. Gronewold Surface acoustic wave sensors in the bioanalytical field: recent

424   trends and challenges Anal. Chim. Acta, 603 (2007), pp. 119–128

425

426   [16] U. Latif, S. Can, O. Hayden, P. Grillberger, F.L. Dickert Sauerbrey and anti-Sauerbrey

427   behavioral studies in QCM sensors – detection of bioanalytes Sens. Actuators B: Chem., 176

428   (2013), pp. 825–830

429   [17]C. Steinem, A. Janshoff Sensors: piezoelectric resonators P. Worsfold, A. Townshend,

430   C. Poole (Eds.), Encyclopedia of Analytical Science (2nd ed.), Elsevier, Oxford (2005), pp.

431   269–276

432   [18] K.K. Reddy, K.V. Gobi Artificial molecular recognition material based biosensor for

433   creatinine by electrochemical impedance analysis Sens. Actuators B: Chem., 183 (2013), pp.

434   356–363.

435   [19] K. Reimhult, K. Yoshimatsu, K. Risveden, S. Chen, L. Ye, A. Krozer

436   Characterization of QCM sensor surfaces coated with molecularly imprinted nanoparticles

437   Biosens. Bioelectron., 23 (2008), pp. 1908–1914

438   [20] B. Khadro, C. Sanglar, A. Bonhomme, A. Errachid, N. Jaffrezic-Renault

439   Molecularly imprinted polymers (MIP) based electrochemical sensor for detection of urea

440   and creatinine Proc. Eng., 5 (2010), pp. 371–374

441   [21] Q. Gai, F. Qu, T. Zhang, Y. Zhang The preparation of bovine serum albumin surface-

442   imprinted superparamagnetic polymer with the assistance of basic functional monomer its

443   application for protein separation J. Chromatogr. A, 1218 (2011), pp. 3489–3495

444   [22] Q. Gai, F. Qu, Y. ZhangThe preparation of BHb-molecularly imprinted gel polymers

445   and its selectivity comparison to BHb and BSA Sep. Sci. Technol., 45 (2010), pp. 2394–2399

446

447   View Record in Scopus | Full Text via CrossRef | Citing articles (9)

448   [23]K.A. Marx Quartz crystal microbalance: a useful tool for studying thin polymer films and

449   complex biomolecular systems at the solution–surface interface

450   Biomacromolecules, 4 (2003), pp. 1099–1120

451   [24] S. Kurosawa, J. Park, H. Aizawa, S. Wakida, H. Tao, K. Ishihara Quartz crystal

452   microbalance immunosensors for environmental monitoring Biosens. Bioelectron., 22 (2006),

453   pp. 473–481

454   [25] T. Zhou, K.A. Marx, M. Warren, H. Schulze, S.J. Braunhut

455   The quartz crystal microbalance as a continuous monitoring tool for the study of endothelial

456   cell surface attachment and growth Biotechnol. Prog., 16 (2000), pp. 268–277

457   [26] Zhou Xue, He Xi-Wen, Chen Lang-Xing, Li Wen-You, Zhang Yu-Kui

458   Optimum conditions of separation selectivity based on molecularly imprinted polymers of

459   bovine serum albumin formed on surface of aminosilica Chin. J. Anal. Chem., 37 (2009), pp.

460   174–180

461   [27] E. Saridakis, S. Khurshid, L. Govada, Q. Phan, D. Hawkins, G.V. Crichlow, E. Lolis,

462   S.M. Reddy, N.E. Chayen Protein crystallization facilitated by molecularly imprinted

463   polymers Proc. Natl. Acad. Sci., 108 (2011), pp. 11081–11086

464

465   Fig. 1.

466   (A) Rebinding capacities (Q) and imprinting factors of MIP_{polyAA} and NIP_{polyAA} hydrogels for several
467   proteins in MilliQ water media: bovine haemoglobin (BHb), bovine serum albumin (BSA), myoglobin
468   (Mb), lysozyme (Lyz), trypsin (Tryp); (B) relative imprinting factors (k) for a range of BHb-
469   MIP_{polyAA} cross-reactants in MilliQ water media. Results illustrate higher MIP selectivities for cognate
470   BHb and the degree of cross-selectivity for other non-template analytes. Data represents
471   mean ± S.E.M., $n = 3$.
472

474   Fig. 2.
475   QCM response to the immersion of polyAA-BHb hydrogel thin-film MIP in 10% (w/v):10% (v/v)
476   SDS:AcOH in order to follow protein elution (arrow indicates time of MIP immersion): (A) impedance
477   (ΔZ), (B) frequency (Δf); QCM responses to BHb (3 mg/mL) loading onto a BHb imprinted polyAA
478   hydrogel thin-film (arrow indicates time of immersion in protein solution): (C) impedance (ΔZ) and (D)
479   frequency (Δf).
480

22

481

482
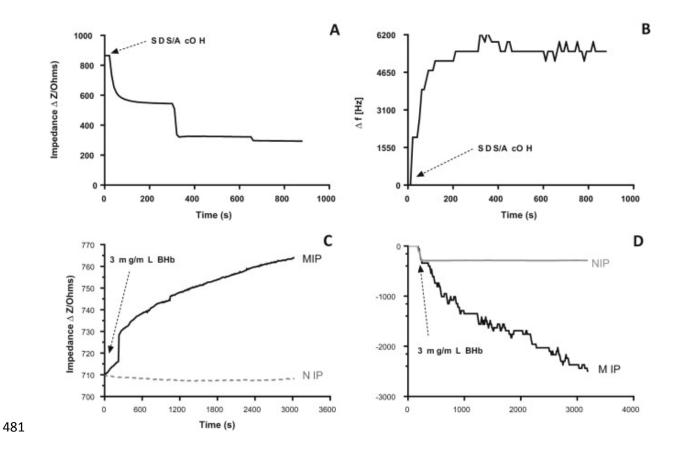
Fig. 3.
QCM frequency shift responses of NiPAm, AA and NHMA polymer MIPs and NIPs to cognate BHb
and non-cognate BSA loading (3 mg/mL) after 5 min of exposure. Data represents
mean ± S.E.M., n = 3.

487
488

489
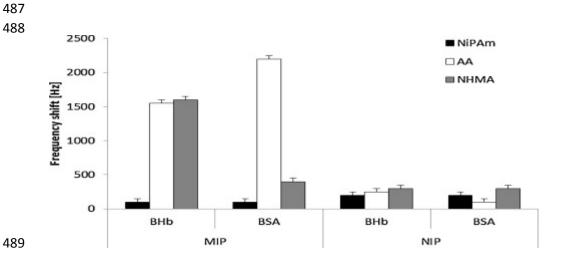
Fig. 4.
Real time QCM impedance responses: (A) direct BHb rebinding and BSA cross-selectivity on a BHb-
MIP$_{polyAA}$; (B) BSA cross-selectivity on a BHb-MIP$_{polyAA}$ followed by BHb rebinding.

493

23

494

495
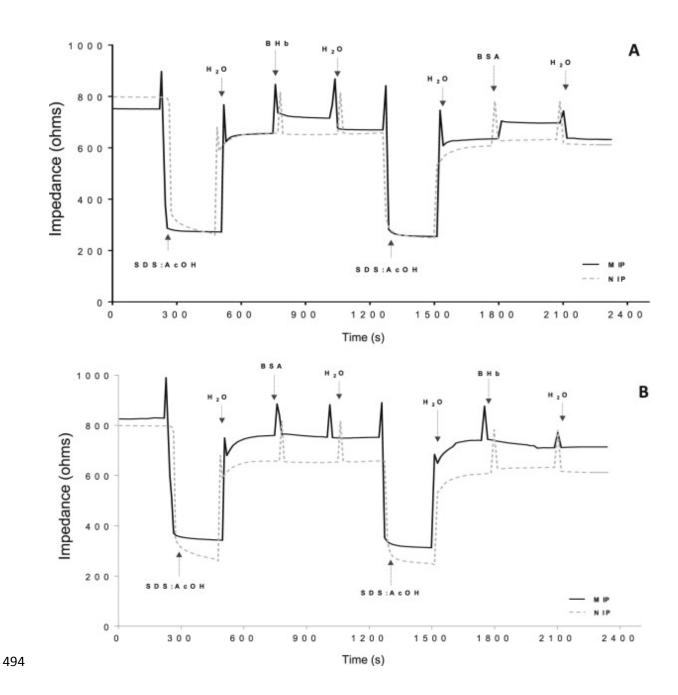
496 Fig. 5.
497 QCM response of functionalised acrylamide BHb MIPs to non-cognate proteins thaumatin (Thau),
498 lysozyme (Lyz), and trypsin (Tryp) after H_2O washes and an SDS:AcOH elute.
499

500

501

502

503

504

505

506

507

508